Open Access

Marcel Böttrich*, Daniel Laqua and Peter Husar

Principle study on the signal connection at transabdominal fetal pulse oximetry

DOI 10.1515/cdbme-2016-0144

Abstract: Transabdominal fetal pulse oximetry is an approach to measure oxygen saturation of the unborn child non-invasively. The principle of pulse oximetry is applied to the abdomen of a pregnant woman, such that the measured signal includes both, the maternal and the fetal pulse curve. One of the major challenges is to extract the shape of the fetal pulse curve from the mixed signal for computation of the oxygen saturation. In this paper we analyze the principle kind of connection of the fetal and maternal pulse curves in the measured signal. A time varying finite element model is used to rebuild the basic measurement environment, including a bulk tissue and two independently pulsing arteries to model the fetal and maternal blood circuit. The distribution of the light fluence rate in the model is computed by applying diffusion equation. From the detectors we extracted the time dependent fluence rate and analyzed the signal regarding its components. The frequency spectra of the signals show peaks at the fetal and maternal basic frequencies. Additional signal components are visible in the spectra, indicating multiplicative coupling of the fetal and maternal pulse curves. We conclude that the underlying signal model of algorithms for robust extraction of the shape of the fetal pulse curve, have to consider additive and multiplicative signal coupling.

Keywords: diffusion theory; fetal pulse oximetry; finite element model; signal coupling.

1 Introduction

Oxygen saturation is seen to be a reliable parameter to assess the wellbeing of human beings as well as unborn children. During late pregnancy and delivery, it happens that the oxygen feed of the fetus is reduced and may lead to hypoxia and severe organ damage [1, 2]. A new approach to detect fetal hypoxia is the transabdominal fetal pulse oximetry. The non-invasive method aims to measure fetal oxygen saturation continuously and to provide a parameter to directly assess the state of health of the fetus. LEDs and photo detectors are placed on the belly of the pregnant woman, such that the photons travel through maternal and fetal tissue before reaching the surface again. The acquired signal consists of both, the fetal and maternal pulse curves. The most important step prior to calculation of the fetal oxygen saturation is the extraction of the fetal pulse curve from the signal mixture [2–4].

This paper investigates the connection of the fetal and maternal pulse curves in the measured signal. The knowledge of coupling and composition of the signal components is the main precondition for separation of the fetal pulse curve from the signal mix. Former works focused on analyzing the photon distribution in static models of the abdomen [3–5]. We constructed a time variant finite-element model to rebuild the basic measurement principle of transabdominal fetal pulse oximetry. Diffusion theory is used to compute the light propagation in the model. Utilizing COMSOL Multiphysics® allows us to do time sweeps and analyze the light fluence rate in a time varying model geometry. The light fluence rate computed at the detector side is modulated by pulsations of both, maternal and fetal, arteries. We analyze the resulting mixed signals to conclude about the superposition and coupling of the maternal and fetal signal components.

2 Methods

2.1 Tissue model with pulsing arteries

The tissue model (shown in Figure 1) is kept as simple as possible to reduce computation time and memory consumption for better handling. Basically it consists of a bulk medium with two arteries embedded. The whole model takes 20 cm × 20 cm × 5 cm (width × height × depth). The maternal and fetal arteries are located in depths of

***Corresponding author: Marcel Böttrich,** Biosignal Processing Group, Technische Universität Ilmenau, Gustav-Kirchhoff Str. 2, 98693 Ilmenau, Germany, E-mail: marcel.boettrich@tu-ilmenau.de
Daniel Laqua and Peter Husar: Biosignal Processing Group, Technische Universität Ilmenau, Gustav-Kirchhoff Str. 2, 98693 Ilmenau, Germany, E-mail: daniel.laqua@tu-ilmenau.de (D. Laqua); peter.husar@tu-ilmenau.de (P. Husar)

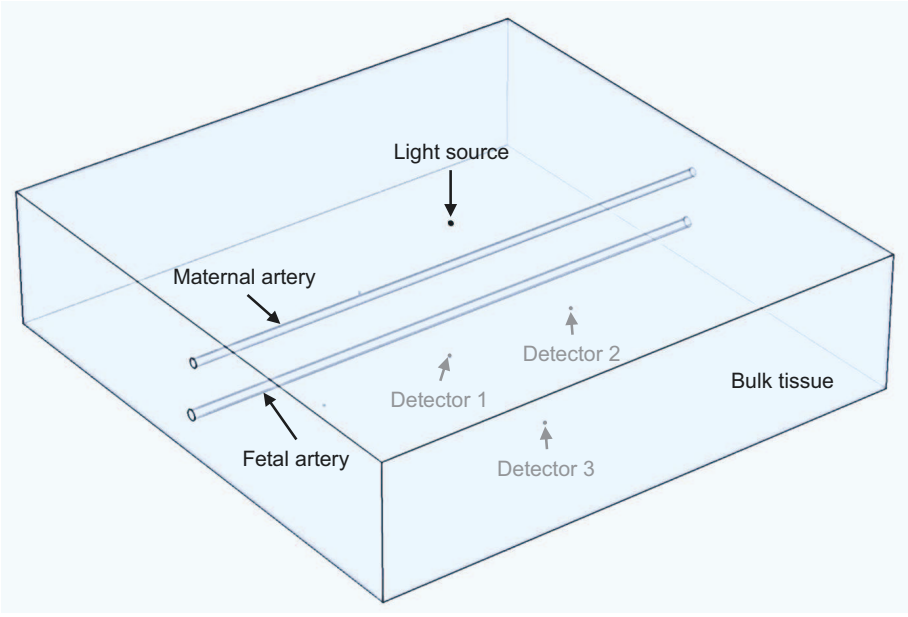

Figure 1: Tissue model with two pulsing arteries embedded. The model consists of a bulk tissue (20 cm × 20 cm × 5 cm) and two artery tubes. The maternal artery and the fetal artery are slightly displaced around the center of the bulk tissue. The light source is placed on top in the middle of the model. Three detectors are on the bottom side.

Table 1: List of the optical properties of the tissue model.

Tissue	μ_s	μ_a	g	n
Bulk	5.0 cm^{-1}	0.08 cm^{-1}	0.80	1.300
Artery	12.0 cm^{-1}	4.70 cm^{-1}	0.99	1.400

The scattering coefficient (μ_s), absorption coefficient (μ_a), anisotropy (g) and refractive index (n) describe the optical characteristics of the tissues.

Table 2: List of the geometrical parameters of the fetal and maternal arteries.

Artery	*A*	*HR*	*Phase*
Maternal	0.1 cm	61 bpm	$\pi/3$ s
Fetal	0.1 cm	113 bpm	0.0 s

A is the amplitude of the oscillation, *HR* the heart rate and *Phase* the phase shift of the cosine function.

1.5 cm and 3.5 cm, respectively, measured from the surface of the bulk medium. The arteries are parallel to each other, but slightly displaced by 0.2 cm symmetrically around the center of the model. The optical parameters, scattering coefficient (μ_s), absorption coefficient (μ_a), anisotropy (g) and refractive index (n), used for light propagation simulation, are listed in Table 1. The surrounding medium of the model is air.

The diameter of the arteries depends on the time parameter. We implemented a cosine function following Equation 1 as a simple approximation of the pulse curve.

$$d = 3 \cdot A + A \cdot cos(2\pi \cdot HR/60 \cdot t + Phase) \quad (1)$$

A is the amplitude of the oscillation, HR the simulated heart rate in *bpm* and *Phase* the phase shift between the fetal and maternal pulsation. The parameters for the pulsation are listed in Table 2.

The light source and detectors are approximated by points. The source point is placed in the center on top of the model, as can be seen in Figure 1. Detector 1 is located on the bottom plane of the model below the source. Detectors 2 and 3, also on the bottom of the model, are slightly displaced from the center, 5 cm following and orthogonally to the direction of the arteries.

2.2 Diffusion theory

The diffusion equation as approximation of the radiative transfer equation is used to compute the light propagation in the tissue model. In comparison to the widely used Monte Carlo method, the diffusion equation allows faster computation of the light fluence distribution in complex geometric models, at similar accuracy [6]. The distribution of the light fluence rate Φ is described by Equation 2 [7, 8].

$$-\nabla \cdot D\nabla\Phi + \mu_a\Phi = q \quad (2)$$

D denotes the diffusion coefficient, μ_a the absorption coefficient and q the source term. The diffusion coefficient

is computed by Equation 3. It can be seen that, beneath the absorption coefficient μ_a, D also depends on the scattering coefficient μ_s and the anisotropy g.

$$D = \frac{1}{3 \cdot (\mu_a + \mu_s(1-g))} = \frac{1}{3 \cdot (\mu_a + \mu_s')} \tag{3}$$

Similar to the anatomy, the model represents several types of tissue with different optical properties. To consider a mismatch of refractive indices between two media, a Robin-type boundary condition is applied. At boundaries, i.e. tissue and air or bulk tissue and blood, the light fluence rate is computed by Equation 4.

$$\Phi + 2AD\vec{n} \bullet \nabla\Phi = 0 \tag{4}$$

A is computed by Equation 5 with $R_0 = (n-1)^2/(n+1)^2$ and $n = n_{in}/n_{out}$. The refractive indices are denoted by n_{in} and n_{out} and the critical angle of total reflection by θ_c [7, 8].

$$A = \frac{\frac{2}{(1-R_0)} - 1 + |cos\theta_c|^3}{1 - |cos\theta_c|^2} \tag{5}$$

In COMSOL Multiphsyics® we use the Helmholtz equation as basic physic to implement these equations and solve for the fluence rate. The time parameter t is sweeped from 0 to 60 s with an interval of 1/60 s, representing a sampling rate of 60 sps. The power of the light source was set to 100 mW.

3 Results

The simulation results show the spatial distribution of the fluence rate in the time varying tissue model. Some examples are shown in Figure 2, with timestamps t = 0.2 s, 0.5 s and 0.8 s. Depicted are slices of the model in its y-z-plane, showing the profile of the arteries. It can be seen that the diameters of the fetal and maternal artery model changes over time, while the light's intensity of the point source is constant. Further, the spatial distribution of the fluence rate slightly varies depending on the current model geometry.

We extracted the fluence rate computed at the bottom side of the model where the two detectors are located. Figure 3 shows the resulting time dependent signal. Depicted is the fluence rate at the detectors relative to the fluence rate at the light source. Basically the two signals show a very similar progress, but differ in their offsets. Detector 1 has a larger offset due to the shortest distance to the light source. It may be assumed that these mixed signals look like two superimposed harmonic oscillations.

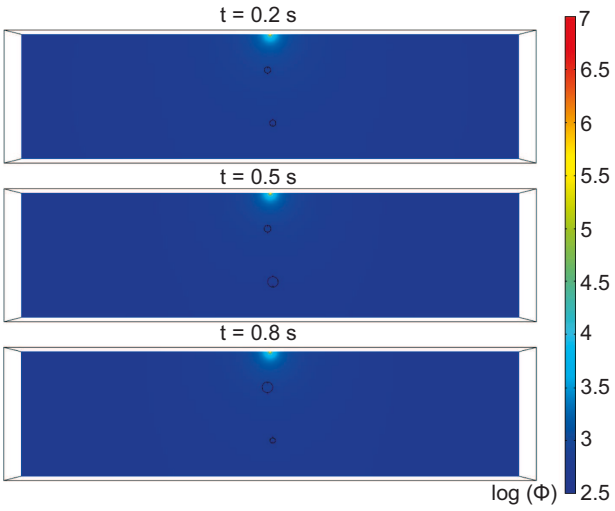

Figure 2: Images of the spatial distribution of the fluence rate for timestamps t = 0.2 s, 0.5 s and 0.8 s. It can be seen that the diameter of the fetal and maternal arteries changes over time, while the source intensity is constant. The fluence distribution slightly changes in dependence on the current geometry of the arteries. For visualization, logarithmic scale is used.

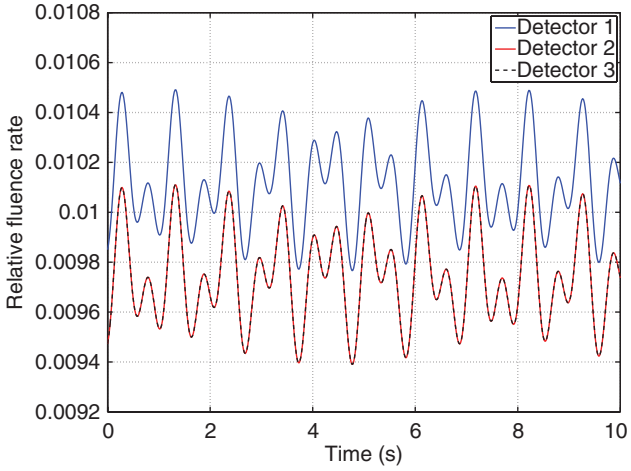

Figure 3: Time series of the light fluence computed at the Detectors 1 (blue), 2 (red) and 3 (black), denoted as mixed signals.

Finally, spectral analysis is done to identify the components of the acquired signals. The magnitude spectra in Figure 4 are generated by using the Fast Fourier Transformation (FFT) and a Blackman window function. The whole signal consists of 3601 samples, so that a frequency resolution of 0.0167 Hz is reached.

The spectra of the three detectors slightly differ in their magnitudes. The main components in the spectrum of the mixed signals are two spectral peaks caused by the arteries, at their basic frequencies of 1.0167 Hz and 1.883 Hz. The weak first harmonic of the maternal artery oscillation is remarkable at 2.0334 Hz. Two additional peaks are at

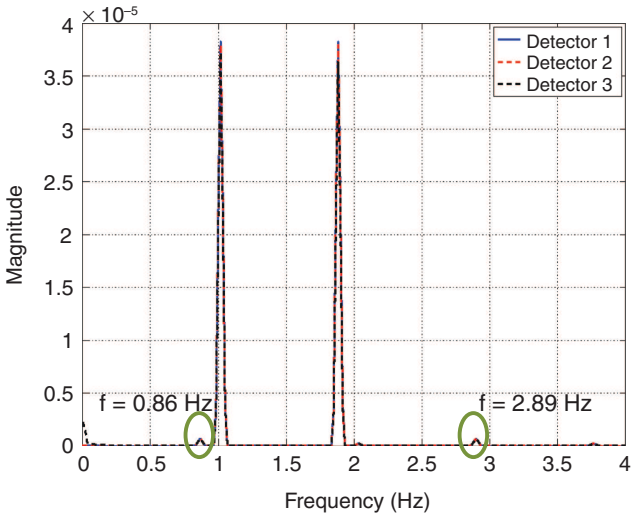

Figure 4: Frequency spectra of the mixed signals, computed from the signals shown in Figure 3. The spectra are computed by using a Blackman window function and the Fast Fourier Transformation (FFT). Beneath the basic oscillations of the arteries (at 1.0167 Hz and 1.883 Hz), two more components exist at frequencies of 0.8664 Hz and 2.899 Hz, respectively.

0.8664 Hz and 2.899 Hz, respectively. The magnitudes of these peaks are about two decades below the magnitude of the main peaks. Due to the simulation, the signals are free of noise.

4 Discussion

The spectra in Figure 4 indicate an additive overlaying of the maternal and fetal pulse curves. A substitution of x and y in Equation 6 by the frequencies of the artery oscillations results in two more components. They are evident in the spectrum at frequencies of 1.883 Hz–1.0167 Hz = 0.8664 Hz and 1.0167 Hz + 1.883 Hz = 2.899 Hz. Thus, these additional peaks result from the multiplicative connection of the maternal and the fetal pulse curves.

$$cos(x) \cdot cos(y) = \frac{1}{2}(cos(x-y) + cos(x+y)) \quad (6)$$

In the consequence, the signal model has to consider a multiplicative connection of the fetal and the maternal pulse curves, following Equation 7.

$$S_{mixed} = a \cdot PC_{mat} + b \cdot PC_{fet} + c \cdot PC_{mat} \cdot PC_{fet} \quad (7)$$

S_{mixed} represents the mixed signal captured by the detector, PC_{mat} and PC_{fet} the maternal and fetal pulse curves weighted by a, b and c, respectively.

The magnitude of the multiplicative connected signal components in the simulation is weak. This indicates that in our simulation setup the amount of light modulated by both arteries before reaching the detector is weak compared to the amount of light modulated by either the maternal or the fetal artery. For Detector 1 and 3 the ratio between the maternal peak and the peak of the multiplicative component is 0.018 and 0.017, respectively, indicating a slightly stronger multiplicative component at Detector 1. In conclusion the ratios among the signal components may change in dependence on the model geometry, i.e. on the position of the arteries, their motion and the position of the light source and detectors. In this study we showed that the fetal and maternal pulse curves are multiplicatively coupled to several extend. Further studies will analyze these components in dependence on the detection quality. A more complex and realistic model of the optical ways in the abdomen will be useful to compare our generated signals to real measurements.

5 Conclusion

This paper analyzes the connection of maternal and fetal signals as they are acquired by non-invasive transabdominal fetal pulse oximetry. Finite element modeling and diffusion equation are conducted to compute spatial distributions of the fluence rate in a tissue model. Two pulsating arteries (maternal and fetal) are embedded in the model, varying their diameter over the time. The light fluence rate is computed for several points at the surface of the model over a time range from 0 to 60 s. A time dependent fluence signal can be extracted and analyzed in frequency domain. Our results show that there is an additive and a multiplicative connection of the fetal and the maternal artery pulsation in the acquired signals. The component resulting from the multiplicative connection in our model geometry is weak. However, following signal processing methods for any separation of the maternal and the fetal pulse curves will consider a signal model with a multiplicative component.

Author's Statement
Research funding: The author state no funding involved. Conflict of interest: Authors state no conflict of interest. Material and Methods: Informed consent: Informed consent is not applicable. Ethical approval: The conducted research is not related to either human or animals use.

References

[1] Choe R, Durduran T, Yu G, Nijland MJ, Chance B, Yodh AG, et al. Transabdominal near infrared oximetry of hypoxic

stress in fetal sheep brain in utero. Proc Natl Acad Sci USA. 2003;100:12950–4.
[2] Zourabian A, Siegel A, Chance B, Ramanujan N, Rode M, Boas DA. Trans-abdominal monitoring of fetal arterial blood oxygenation using pulse oximetry. J Biomed Opt. 2000;5:391–405.
[3] Böttrich M, Ley S, Husar P. Simulation study on the effect of tissue geometries to fluence composition for non-invasive fetal pulse oximetry. 37th Annual International Conference of the IEEE Engineering in Medicine and Biology Society (EMBC); 2015. p. 5122–5.
[4] Gan KB, Zahedi E, Mohd Ali MA. Investigation of optical detection strategies for transabdominal fetal heart rate detection using three-layered tissue model and Monte Carlo simulation. Opt Appl. 2011;41:885–96.
[5] Ley S, Laqua D, Husar P. Simulation of photon propagation in multi-layered tissue for non-invasive fetal pulse oximetry. The 15th International Conference on Biomedical Engineering; 2013. Vol. 43. p. 356–9.
[6] Xu Y, Zhu Q. Comparison of finite element and Monte Carlo simulations for inhomogeneous advanced breast cancer imaging. Proceedings of the COMSOL Conference; 2010.
[7] Li J, Zhu TC. Finite-element modeling of light fluence distribution in prostate during photodynamic therapy. Proceedings of the COMSOL Multiphysics User's Conference; 2005.
[8] Schweiger M, Arridge SR, Hiraoka M, Deply DT. The finite element method for the propagation of light in scattering media: boundary and source conditions. Med Phys. 1995;22:1779–92.